NANO LETTERS

Letter

pubs.acs.org/NanoLett

Can CF_3-Functionalized La@C_{60} Be Isolated Experimentally and Become Superconducting?

Jie Guan and David Tománek*

Physics and Astronomy Department, Michigan State University, East Lansing, Michigan 48824, United States

Supporting Information

ABSTRACT: Superconducting behavior even under harsh ambient conditions is expected to occur in La@C_{60} if it could be isolated from the primary metallofullerene soot when functionalized by CF_3 radicals. We use *ab initio* density functional theory calculations to compare the stability and electronic structure of C_{60} and the La@C_{60} endohedral metallofullerene to their counterparts functionalized by CF_3. We found that CF_3 radicals favor binding to C_{60} and La@C_{60} and have identified the most stable isomers. Structures with an even number m of radicals are energetically preferred for C_{60} and structures with odd m for La@C_{60} due to the extra charge on the fullerene. This is consistent with a wide HOMO−LUMO gap in La@$C_{60}(CF_3)_m$ with odd m, causing extra stabilization in the closed-shell electronic configuration. CF_3 radicals are both stabilizing agents and molecular separators in a metallic crystal, which could increase the critical temperature for superconductivity.

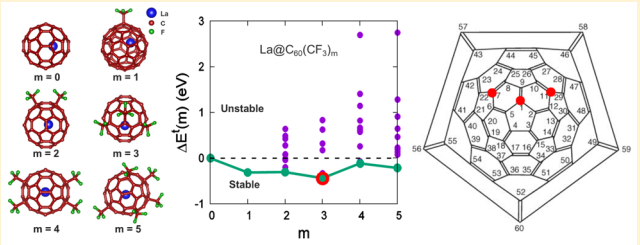

KEYWORDS: *Metallofullerene, La@C_{60}, ab initio, electronic structure*

The discovery of the C_{60} fullerene[1] with a hollow cage structure immediately triggered the question, whether the space inside could be filled by other atoms. This question has been answered affirmatively shortly afterward by successfully encapsulating metal atoms including Li, Na, K, Rb, Sr, Ba, Sc, La, Tc, and U inside M@C_{2n} endohedral fullerenes, also called metallofullerenes.[2−13]

A major reason for the current interest in metallofullerenes such as La@C_{60} is the possibility to observe superconductivity in solid C_{60} that is doped endohedrally rather than exohedrally by three electrons.[14] A molecular crystal formed of isolated and recrystallized La@C_{60} molecules would be electronically related to M_3C_{60} with M representing alkali atoms. In M_3C_{60} crystals, superconductivity with $T_c \lesssim 40$ K has been observed and explained by electron−phonon coupling that is modulated by the lattice constant.[15,16] The same behavior is expected to occur in the isoelectronic La@C_{60} crystal. Unlike alkali-based C_{60} superconductors, La@C_{60} crystals will be stable under ambient or even harsh conditions.

In spite of the fact that fullerene cages of different size favor encapsulation of metal atoms energetically,[3,5,13,17,18] most of the resulting complexes are highly reactive due to their open-shell configuration and form insoluble polymerized solids.[19] Only M@C_{2n} metallofullerenes with large cages[5] ($2n \gtrsim 74$) have been successfully isolated from the raw soot, with M@C_{82} dominating. It has been difficult to extract the most abundant M@C_{60} and M@C_{70} metallofullerenes due to their insolubility in regular fullerene solvents[13,20,21] such as toluene and CS_2. Even though several metallofullerenes with cages as small as C_{60} have been extracted by solvents such as pyridine and aniline,[21−24] it has become a large challenge to separate the M@C_{60} fraction since pyridine and aniline solvents are not suitable for high-performance liquid chromatography (HPLC).[20] Only recently, La@C_{70} and Y@C_{2n} with $2n \geq 60$, functionalized by CF_3 radicals, have been separated using toluene and CS_2 as solvents.[19,25] In this new strategy, the function of trifluoromethyl radicals was to further separate the metallofullerene cages and to chemically stabilize their unstable open-shell electronic configuration.[26] Isolation and crystallization of the more interesting La@C_{60} molecules is currently being attempted.[14]

In view of the possibility to obtain superconducting behavior in crystalline La@C_{60} even under harsh ambient conditions, we provide theoretical support for the experimental effort to solubilize the La@C_{60} endohedral metallofullerene from the primary soot. We made use of *ab initio* density functional theory calculations to compare the stability and electronic structure of the bare C_{60} fullerene and La@C_{60} to their counterparts functionalized by m CF_3 radicals. We found that several CF_3 radicals can form stable bonds to C_{60} and La@C_{60} and have identified the most stable structural isomers for $m \leq 5$. Generally, structures with an even m are energetically preferred for C_{60} and structures with an odd m for La@C_{60} due to the extra three electrons donated by the encapsulated La. This is consistent with our finding that a wide HOMO−LUMO gap opens in La@$C_{60}(CF_3)_m$ molecules with an odd m value,

Received: January 14, 2017
Revised: May 25, 2017
Published: May 30, 2017

DOI: 10.1021/acs.nanolett.7b00185
Nano Lett. 2017, 17, 3402−3408

causing extra stabilization in the closed-shell electronic configuration. The two-fold function of CF_3 radicals as stabilizing agents and molecular separators may help in isolating specific molecules from the primary soot. If La@$C_{60}(CF_3)_m$ could be solubilized and recrystallized, endohedral instead of exohedral doping by three electrons per C_{60} and use of stabilizing CF_3 radicals as spacers may lead to superconductivity with a relatively high T_c achieved by increasing the lattice constant of the molecular crystal.[15,16] We should note that the range of favorable lattice constants is limited since their increase beyond a critical value changes doped C_{60} from a metal to a Mott−Hubbard insulator.[27,28] Even more appealing than changing the lattice constant appears the possibility to remove CF_3 radicals after obtaining La@$C_{60}(CF_3)_m$ in solution and subsequently recrystallize La@C_{60}. Stability even under harsh ambient conditions is expected due to the absence of alkali atoms filling interstitial sites in known M_3C_{60} superconductors. Moreover, the possibility to encapsulate different elemental species provides an additional handle on tuning T_c of M@C_{60} superconductors.[29]

Results. We have used density functional theory (DFT) with the Perdew−Burke−Ernzerhof (PBE)[30] exchange-correlation functional to determine the equilibrium geometry of La@C_{60} and La@$C_{60}(CF_3)_m$ molecules for $m \leq 5$. For a given number m of attached CF_3 radicals, we optimized many different regioisomers, as specified in the Supporting Information, and displayed the most stable structures in Figure 1. Figure 1a displays the bare C_{60} molecule containing a La atom in its equilibrium off-center configuration. As seen in Figure 1b, CF_3 radicals prefer to attach on-top of C atoms in the C_{60} cage. Whereas the adsorption of a single CF_3 radical on the bare C_{60} cage in a metastable geometry is an endothermic process requiring 0.43 eV, presence of La in the La@C_{60} metallofullerene turns this adsorption process exothermic with an energy gain of 0.31 eV. We considered 10 regioisomers for $m = 2$ and display their optimum geometry, the corresponding Schlegel diagram and relative energy in Figure S1 of the Supporting Information, with the most stable geometry given in Figure 1c. These results indicate that CF_3 radicals in the most stable $m = 2$ regioisomer are in para (third neighbor) positions on a single hexagon on the C_{60} surface and that this structure has a C_{2v} symmetry. Other arrangements of the radicals are penalized energetically up to $\lesssim$1 eV. Comparing the relative energies of other regioisomers, we found that CF_3 radicals prefer to be close, but not too close, on the C_{60} surface.

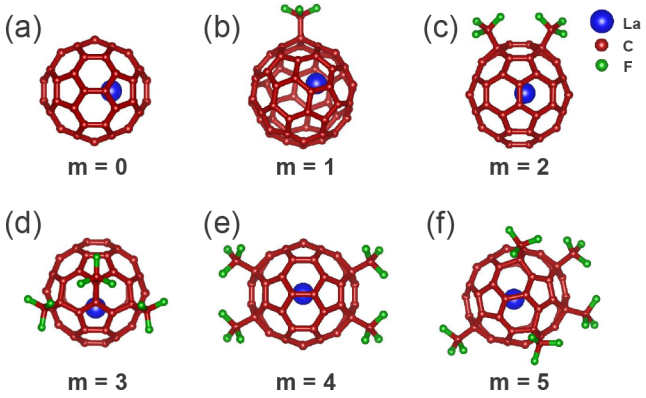

Figure 1. Ball-and-stick models of the optimized structure of the most stable isomers of La@$C_{60}(CF_3)_m$ molecules with (a) $m = 0$, (b) $m = 1$, (c) $m = 2$, (d) $m = 3$, (e) $m = 4$, and (f) $m = 5$.

A very similar picture emerges for $m = 3$ CF_3 radicals adsorbed on La@C_{60}. Six different regioisomers, their relative energies, and the corresponding Schlegel diagrams are presented in Figure S2 of the Supporting Information. As for $m = 2$, the optimum arrangement of CF_3 radicals in the most stable isomer, shown in Figure 1d, is in para position on adjacent hexagonal rings on the C_{60} surface and results in a mirror symmetry for the molecule. The second most stable isomer containing CF_3 radicals separated by five neighbor distances is only ∼0.1 eV less stable than the most stable structure and has a C_3 symmetry. Even though nearest-neighbor arrangements of CF_3 radicals were not considered, other structural candidates incurred an energy penalty of up to $\lesssim$1.3 eV with respect to the most stable isomer.

The structural paradigm changes when increasing the number of CF_3 radicals attached to La@C_{60} to $m = 4$. Among the 10 regioisomers presented in Figure S3 of the Supporting Information, the most stable structure, shown in Figure 1e, contains two pairs of CF_3 radicals in para arrangement on hexagonal rings that are separated by half the circumference of the C_{60} molecule. Another arrangement, with all CF_3 radicals in para arrangement on adjacent hexagonal rings, is energetically the second-best isomer, with its energy only 0.051 eV higher than the most stable structure. The most stable isomer has a C_{2v} symmetry and the second-best isomer only a mirror symmetry.

The structural paradigm for La@$C_{60}(CF_3)_m$ regioisomers with $m = 5$ CF_3 radicals is similar to the $m = 4$ case. The most stable of ten regioisomers, presented in Figure S4 of the Supporting Information and displayed in Figure 1f contains four CF_3 radicals in para arrangement on three adjacent hexagonal rings. The last radical is separated by four neighbor distances from the closest CF_3 radical. It is also possible to arrange all five CF_3 radicals in para positions on four adjacent hexagonal rings, but this highly symmetric regioisomer is less stable by $\lesssim$0.9 eV than the most stable structure.

To find out the preferential number of CF_3 radicals attached to the La@C_{60} molecule, we calculated the energy change $\Delta E^t(m)$ associated with attaching an extra trifluoromethyl radical to the most stable La@$C_{60}(CF_3)_{m-1}$ isomer and display our results in Figure 2. We defined $\Delta E^t(m)$ by

$$\Delta E^t(m) = E_{tot}(m) - E_{tot}^{min}(m-1) - \frac{1}{2}E_{tot}(C_2F_6) \quad (1)$$

$E_{tot}^{min}(m)$ denotes the total energy of the most stable La@$C_{60}(CF_3)_m$ isomer. A negative value of $\Delta E^t(m)$ indicates an exothermic reaction for adsorbing an extra CF_3 radical that had been initially formed by dissociating a hexafluoroethane molecule. $\Delta E^t(0)$ for the bare metallofullerene has been set to zero.

According to our results in Figure 2, it is always possible to find a structural arrangement of CF_3 radicals that would further stabilize the La@C_{60} structure. We find structures with odd number of radicals to be relatively more stable, with $m = 3$ providing the optimum stabilization with $\Delta E^t(3) = -0.44$ eV. In comparison, the stability gain $\Delta E^t(4) = -0.11$ eV upon adsorbing four radicals is much smaller. Equally interesting as the optimum regioisomer is the range of $\Delta E^t(m)$ values for a given m, which is as wide as 3 eV. We should not neglect the fact that functionalization by CF_3 radicals within the raw soot may not always yield the most stable isomers.

DOI: 10.1021/acs.nanolett.7b00185
Nano Lett. 2017, 17, 3402−3408

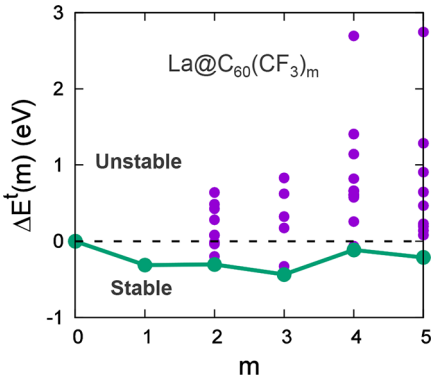

Figure 2. Energy change $\Delta E^t(m)$ associated with attaching an extra trifluoromethyl radical to the most stable La@$C_{60}(CF_3)_{m-1}$ isomer. Negative values denote stable structures, and $\Delta E^t(0)$ is set to zero. $\Delta E^t(m)$ values for the most stable isomers are shown by the larger symbols and are connected by the solid green line to guide the eye.

The even−odd alternation in the $\Delta E^t(m)$ values for the most stable isomers, with odd values referring to higher stability, has been found previously for CF_3-functionalized La@C_{70} and Y@C_{70} molecules.[19,25] The even−odd alternation is also found in CF_3-functionalized fullerenes, which, however, display an energetic preference for an even number of CF_3 radicals.[31,32] The preference of fullerenes for an even number of CF_3 radicals can be explained easily. Attaching an even number of radicals to nominal double-bonds in the fullerene cage converts the C atoms in the double-bond from an sp^2 to an sp^3 configuration, leaving no radical behind. Consequently, an odd number of CF_3 radicals will leave at least one C radical behind, lowering the stability of the structure.

As we will discuss next, an La atom, upon its encapsulation, transfers three electrons to the C_{60} shell, whereas the charge transfer caused by attached CF_3 radicals is significantly smaller. The odd number of electrons added to the shell modifies its electronic structure, resulting in an energetic preference for an odd instead of an even number m of CF_3 radicals attached to C_{60}.

Electronically, there is no difference if the negative charge of the C_{60}^{3-} shell stems from encapsulated La in a hypothetical La@C_{60} or from three alkali atoms that are interstitial in the M_3C_{60} crystal. The electronic structure of the corresponding molecular crystal will be determined by the narrow band formed of the partly occupied LUMO of the C_{60} molecules. Except for a dynamical Jahn−Teller effect, the system should be metallic and superconducting, with T_c depending in the same way on the lattice constant as in the equivalent M_3C_{60} molecular crystal.[16] The present understanding of the origin of superconductivity in alkali-based M_3C_{60} solids is discussed in the Supporting Information.

Plausibilizing the difference between the functionalization of a bare C_{60} fullerene and the La@C_{60} metallofullerene requires understanding the charge redistribution introduced by the encapsulated La atom in C_{60}. We discuss this charge redistribution in detail in the Supporting Information, in

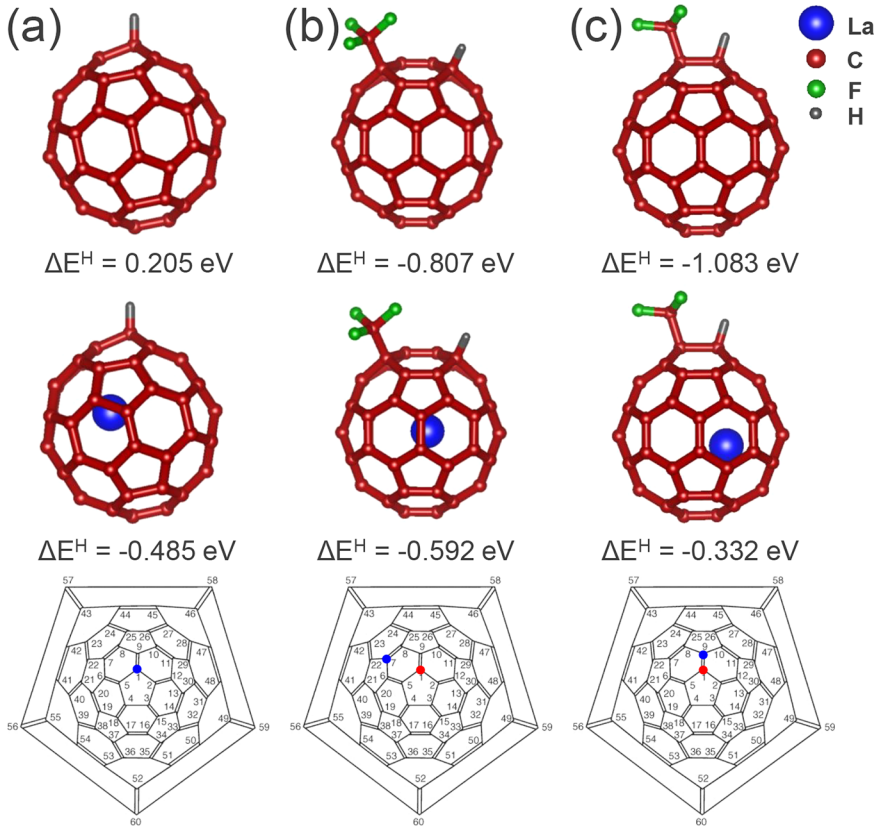

Figure 3. Structural and energetic change caused by hydrogen atom adsorption on (a) C_{60} (top panel) and La@C_{60} (middle panel), and (b,c) on $C_{60}CF_3$ (top panels) and La@$C_{60}CF_3$ (middle panels). The CF_3 radical and the H atom are adsorbed on the same hexagonal ring, occupying (b) para (or third-neighbor) positions or (c) ortho (or first-neighbor) positions. The bottom panels contain the corresponding Schlegel diagrams of C_{60} with the hydrogen sites indicated by the blue and the CF_3 sites by the red dots. ΔE^H denotes the energy change due to hydrogenation, with H_2 as the hydrogen source and negative values denoting an exothermic process.

DOI: 10.1021/acs.nanolett.7b00185
Nano Lett. 2017, 17, 3402−3408

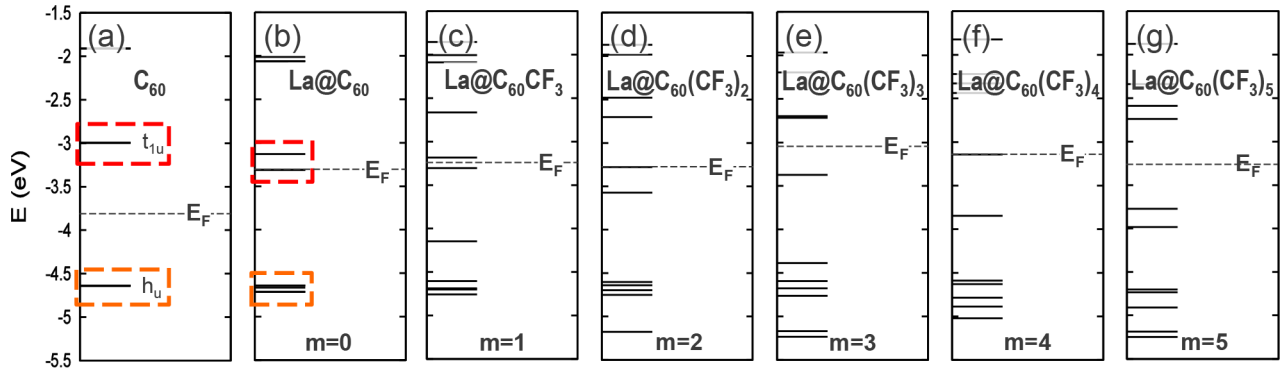

Figure 4. DFT-PBE molecular orbital energies of (a) bare C_{60} molecule, (b) bare La@C_{60} metallofullerene, and La@$C_{60}(CF_3)_m$ functionalized with (c) m = 1, (d) m = 2, (e) m = 3, (f) m = 4, and (g) m = 5 CF_3 radicals. The corresponding (degenerate) energies of the highest occupied and lowest unoccupied states of C_{60} and La@C_{60} are highlighted in (a) and (b).

particular in Figure S1. The essence of our findings is consistent with the Bader charge analysis[33−36] of the bare C_{60} molecule and all metallofullerenes depicted in Figure 1. Independent of the presence and number m of attached CF_3 radicals, we found a net transfer of ∼1.8 electrons from the encapsulated La atom to the C_{60} cage. Restating this finding in a different way, the net charge of the La atom was not affected by the presence of CF_3 radicals carrying a net Bader charge $Q \approx -0.1e$, which was transferred locally from the C_{60} cage alone. In view of the ambiguity to assign a delocalized charge to particular atoms, we may assume that the charge transfer from the La atom to the cage is likely underestimated by the Bader analysis. Comparing to similar systems, where a Bader analysis has been performed,[37,38] we found the enclosed La to be most likely in the 3+ oxidation state, with the C_{60} cage carrying extra three electrons.

The net electron transfer from the encapsulated atom to the surrounding cage is also the cause of the off-center displacement of La by ∼1.2 Å. In DFT-PBE, this symmetry-lowering displacement is associated with an energy gain of ∼3.3 eV. This stabilization energy can be simply explained by the electrostatic polarization energy gain caused by a point charge moving off-center inside a spherical metallic shell, as discussed previously for other metallofullerenes.[39,40] Using +3e as the net charge of the enclosed La and 3.5 Å as the radius of the C_{60} shell, we estimated in this way an energy gain of 1.7 eV, the same order of magnitude as the value obtained in the DFT calculation.

If the reason for altering the energetic preference from an even to an odd number of attached CF_3 radicals is leaving or not leaving a C radical behind, then a single chemisorbed H atom chemisorbed on the same double-bond as a lone CF_3 radical may reverse this preference. To investigate this possibility, we studied the structural and energetic changes associated with the chemisorption of a hydrogen atom on bare and CF_3-functionalized fullerenes and metallofullerenes and present our results in Figure 3.

We defined the energy change ΔE^H associated with attaching a single H atom to a bare of CF_3-functionalized fullerene C_{60} or metallofullerene La@C_{60}, denoted by R, by

$$\Delta E^H = E_{tot}(H/R) - E_{tot}(R) - \frac{1}{2}E_{tot}(H_2) \quad (2)$$

A negative value of ΔE^H indicates that the adsorption of an H atom, which had initially been formed by dissociating an H_2 molecule, is exothermic.

The top row in Figure 3 describes different ways of chemically functionalizing a C_{60} cage. The positive value of ΔE^H in the top panel of Figure 3a indicates that hydrogen prefers not to adsorb on the bare C_{60} cage, as discussed previously for carbon nanotubes and fullerenes.[41,42] This behavior changes in the presence of an adsorbed CF_3 radical, which modifies the electronic structure of the cage. Noting that adsorption of an isolated H atom or an isolated CF_3 radical on the cage are both endothermic processes, it is remarkable that the coadsorption of CF_3 and H turns strongly exothermic, as seen in the top panels of Figures 3b,c. As anticipated above and seen in the top panel of Figure 3c, the largest energy gain occurs when the adsorbates attach to the same double-bond on the cage, in ortho arrangement on the same hexagonal ring, changing the configuration of the adjacent C atoms from sp^2 to sp^3 and leaving no C radical behind. Somewhat less favorable is coadsorption in a para arrangement on the same hexagon, shown in the top panel of Figure 3b. The adsorption sites and the differences in local bonding mentioned above are best discussed using the Schlegel diagrams in the bottom panels of Figure 3.

The energetics of chemical functionalization changes completely when a La atom becomes enclosed in the C_{60} cage. Since the adsorption of an isolated H atom or an isolated CF_3 radical become exothermic processes on La@C_{60}, it is not surprising that all values of ΔE^H are negative, as seen in the second row of Figure 3. This means, in other words, that hydrogenation of La@$C_{60}(CF_3)_m$ is always exothermic, irrespective of the presence of CF_3 radicals on the surface. Unlike in the top row, the three values of ΔE^H in the second row are much more similar: adsorbing an extra CF_3 radical next to a preadsorbed H atom lowers the energy by ∼0.1 eV in the para configuration and raises it by ∼0.2 eV in the ortho configuration. We note the small energetic preference for the para configuration in this case, which is reminiscent of the most stable regioisomer of La@$C_{60}(CF_3)_2$ shown in Figure 1c.

The change in behavior can be attributed to the three electrons donated to the C_{60} cage from the encapsulated La atom. Each of these extra electrons can be partly transferred to the electronegative CF_3 radical and participate in bonding, leaving no C radical behind. This is the reason behind our finding in Figure 2 that La@$C_{60}(CF_3)_m$ is most stable for m = 3.

As suggested by the above results, electronic structure plays the key role in determining both the stability and reactivity of fullerenes and (functionalized) metallofullerenes. The electronic eigenstates of the optimized bare C_{60} molecule and of

DOI: 10.1021/acs.nanolett.7b00185
Nano Lett. 2017, 17, 3402−3408

the La@$C_{60}(CF_3)_m$ molecules with $0 \leq m \leq 5$, depicted in Figure 1, are presented in Figure 4. The energy eigenvalues are the Kohn−Sham energies of our DFT-PBE calculations, which are known to underestimate the HOMO−LUMO gap.

As seen in Figure 4a, the calculated gap between the five-fold degenerate h_u HOMO and the three-fold degenerate t_{1u} LUMO of the highly symmetric C_{60} molecule is ∼1.6 eV wide, slightly lower than the observed value[43] of 1.9 eV. The calculated electronic spectrum of La@C_{60} is shown in Figure 4b. As expected, the off-center displacement of the La atom reduces the symmetry and the degeneracy of electronic states. For the sake of simple comparison, we highlighted the occupied h_u state of C_{60} and the corresponding occupied eigenstates in La@C_{60} by the orange-bounded rectangle. As seen in Figure 4b, the symmetry lowering due to the off-center displacement of La splits the h_u state of C_{60} into three closely spaced states, two of which are doubly degenerate. More interesting is the behavior of the initially unfilled t_{1u} state in the C_{60} molecule, which splits into two states, as highlighted by the red-bounded rectangle in Figures 4a,b. The lower of these states in La@C_{60} is doubly degenerate and acquires three extra electrons from the enclosed La atom. Consequently, this partly occupied state defines the Fermi level and provides a metallic character for the La@C_{60} molecule. The significant fundamental band gap is responsible for the high stability and low reactivity of the C_{60} molecule, whereas a vanishing band gap renders La@C_{60} highly reactive. To better understand the effect of the encapsulated La atom on the electronic structure of the La@C_{60} molecule, we discuss the frontier states near the Fermi level of C_{60} and La@C_{60} molecules in the Supporting Information.

For La@$C_{60}(CF_3)_m$ metallofullerenes functionalized with $m \geq 1$ CF_3 radicals, the eigenstates undergo a complex change and can no longer be simply compared to those of the bare C_{60} molecule. Comparing our results in Figures 4b−g, we find zero fundamental band gap in molecules with an even number m of CF_3 radicals and a nonzero band gap if m is odd. This finding suggests that La@C_{60} molecules with an odd number of CF_3 radicals should be more stable, in accord with our previous findings based on total energy calculations. Among La@$C_{60}(CF_3)_m$ molecules, we found the largest HOMO−LUMO gap $E_g \approx 1.0$ eV for $m = 5$, followed by $E_g \approx 0.7$ eV for $m = 3$ and a very small value $E_g \approx 0.1$ eV for $m = 1$. Consequently, we expect metallofullerenes with $m = 3$ and $m = 5$ CF_3 radicals to be most abundant and easiest to separate from the primary soot, as also suggested by preliminary experimental data.[14] Metallofullerenes with an even number of CF_3 radicals have unpaired electrons at the Fermi level, which makes these molecules more reactive and less stable.

All molecules discussed above will be further stabilized when crystallizing in a lattice. We performed corresponding calculations and found that, same as C_{60} molecules, the metallofullerenes prefer the close-packed fcc lattice and also found no indication of dimerization in the lattice. One issue that is typically neglected when judging the stability of crystalline lattices using single-molecule description is the effect of the long-range dipole−dipole interaction. To judge the importance of this effect, we performed DFT-PBE calculations for selected fullerene and metallofullerene lattices. Even though the PBE exchange-correlation functional does not describe the van der Waals interaction accurately, such calculations still provide an adequate description of the charge redistribution and dipole−dipole interaction. C_{60} molecules, carrying no dipole moment, crystallize preferably in an fcc lattice with a nearest-neighbor distance of 10.83 Å, gaining energetically ∼0.06 eV per molecule. According to our Bader charge analysis, La@C_{60} metallofullerenes carry a dipole moment $p = 3.3$ D and crystallize in an fcc lattice with a slightly reduced nearest-neighbor distance of 10.72 Å, gaining ∼0.10 eV per molecule. The stabilization of the La@C_{60} lattice with respect to crystalline C_{60} lattice, however small, benefits to a large degree from the long-range dipole−dipole interaction since an fcc lattice of $p = 3.3$ D point dipoles should be stabilized by a comparable energy of ∼0.06 eV/molecule. We have furthermore found that functionalization of the La@C_{60} metallofullerene by CF_3 radicals increases the molecular dipole moment but also increases the nearest-neighbor distance. In the fcc lattice of La@$C_{60}CF_3$ molecules with a dipole moment $p \approx 12.4$ D, the nearest-neighbor distance increases to 11.72 Å and the stabilization in the lattice changes to ∼0.09 eV/molecule. Similarly, in the fcc lattice of the most stable La@$C_{60}(CF_3)_2$ molecules with a dipole moment $p \approx 18.9$ D, the nearest-neighbor distance changes to 11.68 Å and the stabilization in the lattice changes to ∼0.10 eV/molecule. The above DFT-PBE values of the lattice stabilization energy in CF_3-functionalized metallofullerenes are one order of magnitude smaller than estimates based on the interaction of point dipoles. Our overall finding is that long-range dipole−dipole interaction is of secondary importance for these lattices.

Conclusions. In summary, exploring the possibility to obtain superconducting behavior in crystalline La@C_{60} even under harsh ambient conditions, we provided theoretical support for the experimental effort to solubilize the La@C_{60} endohedral metallofullerene from the primary soot. We used *ab initio* density functional theory calculations to compare the stability and electronic structure of the bare C_{60} fullerene and La@C_{60} to their counterparts functionalized by m CF_3 radicals. We found that several CF_3 radicals can form stable bonds to C_{60} and La@C_{60} and have identified the most stable structural isomers for $m \leq 5$. Generally, structures with an even m are energetically preferred for C_{60} and structures with an odd m for La@C_{60} due to the extra three electrons donated by the encapsulated La. This is consistent with our finding that a wide HOMO−LUMO gap opens in La@$C_{60}(CF_3)_m$ molecules with an odd m value, causing extra stabilization in the closed-shell electronic configuration. We also addressed the possibility of a single hydrogen atom adsorbing at a C radical site in La@$C_{60}(CF_3)_m$, which would further stabilize the open-shell configuration for odd m values and reduce the even/odd alternation in stability. We found that the two-fold function of CF_3 radicals as stabilizing agents and molecular separators may help in isolating specific molecules from the primary soot. If La@$C_{60}(CF_3)_m$ could be solubilized and recrystallized, endohedral instead of exohedral doping by three electrons per C_{60} and use of stabilizing CF_3 radicals as spacers may lead to superconductivity with a relatively high T_c achieved by optimizing the lattice constant of the molecular crystal. Stability even under harsh ambient conditions should then be expected due to the absence of alkali atoms filling the interstitial sites in known M_3C_{60} superconductors.

Computational Techniques. We utilized *ab initio* density functional theory (DFT) as implemented in the VASP code[44−46] to optimize the structure of C_{60} and La@$C_{60}(CF_3)_m$ functionalized with $0 \leq m \leq 5$ CF_3 radicals and obtained the total energy as well as the electronic structure for these systems. We used projector-augmented-wave (PAW) pseudopotentials[47] and the Perdew−Burke−Ernzerhof (PBE)[30]

DOI: 10.1021/acs.nanolett.7b00185
Nano Lett. 2017, 17, 3402−3408

exchange-correlation functional. All isolated structures have been represented using periodic boundary conditions and separated by a 12 Å thick vacuum region, so that no band dispersion could be detected. We used 500 eV as the electronic kinetic energy cutoff for the plane-wave basis and a total energy difference between subsequent iterations below 10^{-5} eV as the criterion for reaching self-consistency. All geometries have been optimized using the conjugate-gradient method[48] until none of the residual Hellmann−Feynman forces exceeded 10^{-2} eV/Å.

■ ASSOCIATED CONTENT

Supporting Information

The Supporting Information is available free of charge on the ACS Publications website at DOI: 10.1021/acs.nanolett.7b00185.

Additional information is provided regarding the origin of superconductivity in alkali-based M_3C_{60} solids, charge distribution in the frontier states of pristine C_{60} and La@C_{60} molecules, and the equilibrium structure and stability of different La@$C_{60}(CF_3)_m$ regioisomers (PDF)

■ AUTHOR INFORMATION

Corresponding Author

*E-mail: tomanek@pa.msu.edu.

ORCID

David Tománek: 0000-0003-1131-4788

Notes

The authors declare no competing financial interest.

■ ACKNOWLEDGMENTS

We would like to acknowledge useful discussions with Hisanori Shinohara, who inspired this study and advised us of experimental progress in his group, and with Zhongqi Jin. This study was supported by the NSF/AFOSR EFRI 2-DARE grant number #EFMA-1433459. Computational resources have been provided by the Michigan State University High Performance Computing Center.

■ REFERENCES

(1) Kroto, H. W.; Heath, J. R.; O'Brien, S. C.; Curl, R. F.; Smalley, R. E. *Nature* **1985**, *318*, 162−163.

(2) Heath, J. R.; O'Brien, S. C.; Zhang, Q.; Liu, Y.; Curl, R. F.; Tittel, F. K.; Smalley, R. E. *J. Am. Chem. Soc.* **1985**, *107*, 7779−7780.

(3) Chai, Y.; Guo, T.; Jin, C.; Haufler, R. E.; Chibante, L. P. F.; Fure, J.; Wang, L.; Alford, J. M.; Smalley, R. E. *J. Phys. Chem.* **1991**, *95*, 7564−7568.

(4) Haufler, R. E.; et al. *J. Phys. Chem.* **1990**, *94*, 8634−8636.

(5) Shinohara, H.; Yamaguchi, H.; Hayashi, N.; Sato, H.; Ohkohchi, M.; Ando, Y.; Saito, Y. *J. Phys. Chem.* **1993**, *97*, 4259−4261.

(6) Tellgmann, R.; Krawez, N.; Lin, S.-H.; Hertel, I. V.; Campbell, E. E. B. *Nature* **1996**, *382*, 407−408.

(7) Campbell, E.; Tellgmann, R.; Krawez, N.; Hertel, I. *J. Phys. Chem. Solids* **1997**, *58*, 1763−1769.

(8) Almeida Murphy, T.; Pawlik, T.; Weidinger, A.; Höhne, M.; Alcala, R.; Spaeth, J.-M. *Phys. Rev. Lett.* **1996**, *77*, 1075−1078.

(9) Knapp, C.; Dinse, K.-P.; Pietzak, B.; Waiblinger, M.; Weidinger, A. *Chem. Phys. Lett.* **1997**, *272*, 433−437.

(10) Mauser, H.; Hirsch, A.; van Eikema Hommes, N. J. R.; Clark, T.; Pietzak, B.; Weidinger, A.; Dunsch, L. *Angew. Chem., Int. Ed. Engl.* **1997**, *36*, 2835−2838.

(11) Hirata, T.; Hatakeyama, R.; Mieno, T.; Sato, N. *J. Vac. Sci. Technol., A* **1996**, *14*, 615−618.

(12) Weck, P. F.; Kim, E.; Czerwinski, K. R.; Tománek, D. *Phys. Rev. B: Condens. Matter Mater. Phys.* **2010**, *81*, 125448.

(13) Shinohara, H. *Rep. Prog. Phys.* **2000**, *63*, 843.

(14) Shinohara, H. Private communication.

(15) Schluter, M.; Lannoo, M.; Needels, M.; Baraff, G. A.; Tomanek, D. *Phys. Rev. Lett.* **1992**, *68*, 526−529.

(16) Schluter, M.; Lannoo, M.; Needels, M.; Baraff, G. A.; Tomanek, D. *J. Phys. Chem. Solids* **1992**, *53*, 1473−1485.

(17) Yamamoto, K.; Funasaka, H.; Takahashi, T.; Akasaka, T. *J. Phys. Chem.* **1994**, *98*, 2008−2011.

(18) Kikuchi, K.; Suzuki, S.; Nakao, Y.; Nakahara, N.; Wakabayashi, T.; Shiromaru, H.; Saito, K.; Ikemoto, I.; Achiba, Y. *Chem. Phys. Lett.* **1993**, *216*, 67−71.

(19) Wang, Z.; Nakanishi, Y.; Noda, S.; Niwa, H.; Zhang, J.; Kitaura, R.; Shinohara, H. *Angew. Chem., Int. Ed.* **2013**, *52*, 11770−11774.

(20) Ogawa, T.; Sugai, T.; Shinohara, H. *J. Am. Chem. Soc.* **2000**, *122*, 3538−3539.

(21) Kubozono, Y.; Noto, T.; Ohta, T.; Maeda, H.; Kashino, S.; Emura, S.; Ukita, S.; Sogabe, T. *Chem. Lett.* **1996**, *25*, 453−454.

(22) Wang, L.; Alford, J.; Chai, Y.; Diener, M.; Zhang, J.; McClure, S.; Guo, T.; Scuseria, G.; Smalley, R. *Chem. Phys. Lett.* **1993**, *207*, 354−359.

(23) Wang, L.-S.; Alford, J. M.; Chai, Y.; Diener, M.; Smalley, R. E. *Z. Phys. D: At., Mol. Clusters* **1993**, *26*, 297−299.

(24) Kubozono, Y.; Ohta, T.; Hayashibara, T.; Maeda, H.; Ishida, H.; Kashino, S.; Oshima, K.; Yamazaki, H.; Ukita, S.; Sogabe, T. *Chem. Lett.* **1995**, *24*, 457−458.

(25) Wang, Z.; Aoyagi, S.; Omachi, H.; Kitaura, R.; Shinohara, H. *Angew. Chem., Int. Ed.* **2016**, *55*, 199−202.

(26) Diener, M. D.; Alford, J. M. *Nature* **1998**, *393*, 668−671.

(27) Ganin, A. Y.; Takabayashi, Y.; Jeglič, P.; Arčon, D.; Potočnik, A.; Baker, P. J.; Ohishi, Y.; McDonald, M. T.; Tzirakis, M. D.; McLennan, A.; Darling, G. R.; Takata, M.; Rosseinsky, M. J.; Prassides, K. *Nature* **2010**, *466*, 221−225.

(28) Nomura, Y.; Sakai, S.; Capone, M.; Arita, R. *Science Adv.* **2015**, *1*, e1500568.

(29) Takeda, A.; Yokoyama, Y.; Ito, S.; Miyazaki, T.; Shimotani, H.; Yakigaya, K.; Kakiuchi, T.; Sawa, H.; Takagi, H.; Kitazawa, K.; Dragoe, N. *Chem. Commun.* **2006**, 912−914.

(30) Perdew, J. P.; Burke, K.; Ernzerhof, M. *Phys. Rev. Lett.* **1996**, *77*, 3865−3868.

(31) Darwish, A. D.; Abdul-Sada, A. K.; Avent, A. G.; Martsinovich, N.; Street, J. M.; Taylor, R. *J. Fluorine Chem.* **2004**, *125*, 1383−1391.

(32) Dorozhkin, E. I.; Goryunkov, A. A.; Ioffe, I. N.; Avdoshenko, S. M.; Markov, V. Y.; Tamm, N. B.; Ignat'eva, D. V.; Sidorov, L. N.; Troyanov, S. I. *Eur. J. Org. Chem.* **2007**, *2007*, 5082−5094.

(33) Henkelman, G.; Arnaldsson, A.; Jónsson, H. *Comput. Mater. Sci.* **2006**, *36*, 354−360.

(34) Sanville, E.; Kenny, S. D.; Smith, R.; Henkelman, G. *J. Comput. Chem.* **2007**, *28*, 899−908.

(35) Tang, W.; Sanville, E.; Henkelman, G. *J. Phys.: Condens. Matter* **2009**, *21*, 084204.

(36) Yu, M.; Trinkle, D. R. *J. Chem. Phys.* **2011**, *134*, 064111.

(37) Lee, Y.-L.; Kleis, J.; Rossmeisl, J.; Morgan, D. *Phys. Rev. B: Condens. Matter Mater. Phys.* **2009**, *80*, 224101.

(38) Yang, T.; Dong, B.; Wang, J.; Zhang, Z.; Guan, J.; Kuntz, K.; Warren, S. C.; Tománek, D. *Phys. Rev. B: Condens. Matter Mater. Phys.* **2015**, *92*, 125412.

(39) Wang, Y.; Tomanek, D.; Ruoff, R. S. *Chem. Phys. Lett.* **1993**, *208*, 79−85.

(40) Li, Y. S.; Tomanek, D. *Chem. Phys. Lett.* **1994**, *221*, 453−458.

(41) Miller, G.; Kintigh, J.; Kim, E.; Weck, P.; Berber, S.; Tomanek, D. *J. Am. Chem. Soc.* **2008**, *130*, 2296−2303.

(42) Berber, S.; Tománek, D. *Phys. Rev. B: Condens. Matter Mater. Phys.* **2009**, *80*, 075427.

(43) Weaver, J. H.; Martins, J. L.; Komeda, T.; Chen, Y.; Ohno, T. R.; Kroll, G. H.; Troullier, N.; Haufler, R. E.; Smalley, R. E. *Phys. Rev. Lett.* **1991**, *66*, 1741−1744.

(44) Kresse, G.; Furthmüller, J. *Phys. Rev. B: Condens. Matter Mater. Phys.* **1996**, *54*, 11169−11186.

DOI: 10.1021/acs.nanolett.7b00185
Nano Lett. 2017, 17, 3402−3408

(45) Kresse, G.; Hafner, J. *Phys. Rev. B: Condens. Matter Mater. Phys.* **1993**, *47*, 558−561.
(46) Kresse, G.; Hafner, J. *Phys. Rev. B: Condens. Matter Mater. Phys.* **1994**, *49*, 14251−14269.
(47) Kresse, G.; Joubert, D. *Phys. Rev. B: Condens. Matter Mater. Phys.* **1999**, *59*, 1758−1775.
(48) Hestenes, M. R.; Stiefel, E. *J. Res. Natl. Bur. Stand.* **1952**, *49*, 409−436.

DOI: 10.1021/acs.nanolett.7b00185
Nano Lett. 2017, 17, 3402−3408